

# APPLICATION OF STOCHASTIC AND ARTIFICIAL INTELLIGENCE METHODS FOR NUCLEAR MATERIAL IDENTIFICATION

Sara Pozzi  
Department of Nuclear Engineering  
Polytechnic of Milan, Italy  
e-mail: pozzi@ipmce7.cesnef.polimi.it

F. J. Segovia  
Facultad Informatica  
Universided Politecnica de Madrid  
Madrid, Spain  
e-mail: fsegovia@fi.upm.es

## ABSTRACT

Nuclear materials safeguard necessitates the use of non-destructive methods to determine the attributes of fissile samples enclosed in special, non-accessible containers. To this end, a large variety of methods has been developed at the Oak Ridge National Laboratory (ORNL) and elsewhere.<sup>1,2</sup> Active non-destructive assay evolved based on the use of an interrogation source emitting neutrons and gamma rays, whose scope is that of inducing fission in the fissile material within the sample. Usually, a given set of statistics of the stochastic neutron-photon coupled field, such as source-detector, detector-detector cross correlation functions, and multiplicities are measured over a range of known samples to develop calibration algorithms. In this manner, the attributes of unknown samples can be inferred by the use of the calibration results. The goal of this paper is to develop an artificial intelligence approach to this problem whereby neural networks (NNs) and genetic programming (GP) algorithms are used for sample identification purposes. To this end, a number of Monte Carlo simulations were performed to obtain source-detector time-dependent cross correlation functions for a set of uranium metal samples of different shapes, masses, and enrichments. A number of features were identified and extracted from the cross correlation functions and effectively related to the sample's mass and enrichment.

## 1. INTRODUCTION

The aim of sample identification in nuclear safeguards is to determine the relationship between selected features of the measurement and the sample's attributes. The features are then combined in the construction of an optimal identification algorithm. In this paper we present an artificial intelligence (AI) approach to this problem whereby neural networks (NN) and genetic programming (GP) algorithms are used for sample identification purposes. To this end, the time-dependent MCNP-DSP<sup>3</sup> Monte Carlo code has been used to simulate the neutron-photon interrogation of sets of uranium metal samples by a <sup>252</sup>Cf-source. The resulting sets of source-detector correlation functions,  $R_{12}(\tau)$  as a function of the time delay,  $\tau$ , served as a data-base for the training and testing of the AI algorithms.

The organization of this paper is as follows: Section 2 describes the Monte-Carlo simulations of source-detector cross correlation functions for a set of uranium metallic samples interrogated by the neutrons and photons from a <sup>252</sup>Cf source. From this database, a set of features is extracted in Section 3. The use of neural networks (NN) and genetic programming to provide sample mass and enrichment values from the input sets of features are illustrated in Sections 4 and 5, respectively. Section 6 is a comparison of the results, while Section 7 is a brief summary of the work.

## 2. <sup>252</sup>Cf-SOURCE-DRIVEN SIMULATIONS

In the <sup>252</sup>Cf-source-driven measurement the source undergoes spontaneous fission emitting neutrons and gamma rays. The timing of each spontaneous fission event is recorded in appropriate time bins. If fissile material is present inside the sample to be analyzed, the neutrons emitted by the source will initiate fission chains. Neutrons and gamma rays from the source as well as those eventually emitted by the fissile system are measured with two fast plastic scintillation detectors. The detection times are also recorded in time bins of 1 ns. The source is located at 25.4 cm from the center of the uranium metal sample at a height of 25.4 cm from the center of the sample.

Simulations were performed with cylindrical and spherical samples of seven different masses (8 kg, 10 kg, 12 kg, 14 kg, 16 kg, 18 kg, and 20 kg). The different masses were obtained by increasing the sample radius, both in the case of the cylinders (in which case the height was kept constant at 20 cm) and in that of the spheres. For each mass, four different enrichments were tested ranging from depleted to highly enriched (0.2 wt% <sup>235</sup>U, 36.0 wt% <sup>235</sup>U, 50.0 wt% <sup>235</sup>U, and 93.15 wt% <sup>235</sup>U), giving a total of 30 simulations for the cylindrical samples and 28 for the spherical ones. An additional simulation run with no sample between source and detectors will be referred to as the void simulation.

The source-detectors cross-correlation functions [ $R_{12}(\tau)$ ] are generated by correlation of the source signal with the combined signal from the two detectors, and normalizing to the source count rate to remove the dependence on the source.

In Figure 2.1 the cross-correlation  $R_{12}(\tau)$  as a function of the delay time between source fission and corresponding detection is shown for cylinders of varying enrichment and fixed mass (20 kg). The curve consists of two major components: a first peak due to directly transmitted gamma rays from the <sup>252</sup>Cf fission (the photo peak), and a second, broader peak due to directly transmitted and scattered neutrons from the source and secondary neutrons and gamma rays from fission induced inside the uranium sample. As it can be seen from the figure, the directly transmitted gamma rays are not very sensitive to the fissile mass since gamma ray attenuation is not related to fission. On the other hand, the second peak of the cross-correlation function depends strongly on enrichment.

In the first part of the second peak the curves show similar behavior for time lags below 20 ns, since the directly transmitted neutrons and secondary photons are not strongly dependent on enrichment. Above time lags of about 20 ns, the peak broadens: neutrons generated by secondary fission inside the fissile material increase and the number of neutron generations increases. The total path covered by the neutrons before a detection event occurs also increases.

Figure 2.2 shows the source-detectors cross-correlation function in the case of cylinders of varying mass and constant enrichment (36 wt% <sup>235</sup>U). In this case, both the gamma peak and the secondary peak height are inversely related to mass: as the sample mass increases, so does the attenuation of gamma rays and neutrons. A similar relationship was found with other values of enrichment.

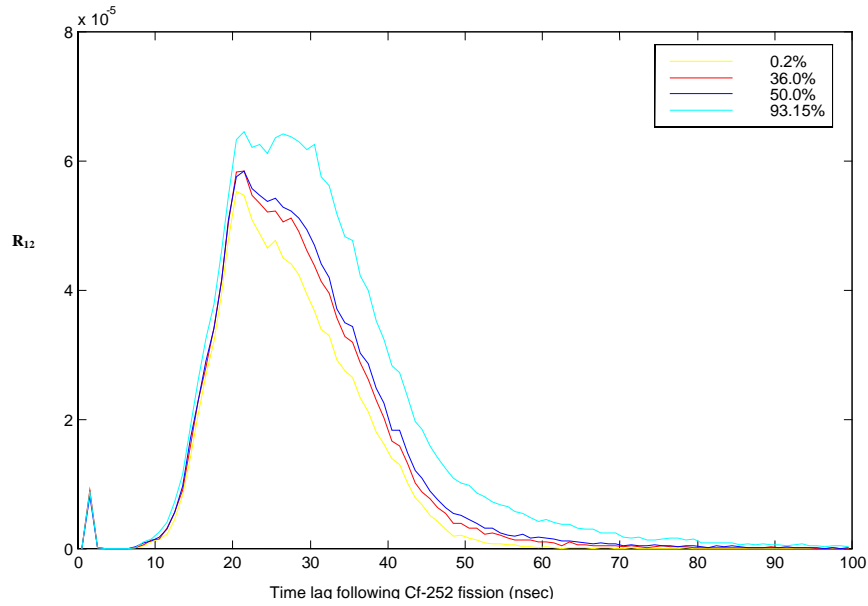


Fig. 2.1. Source-Detectors Cross-Correlation Functions for Uranium Cylinders of Different Enrichments and Fixed Mass (20 Kg).

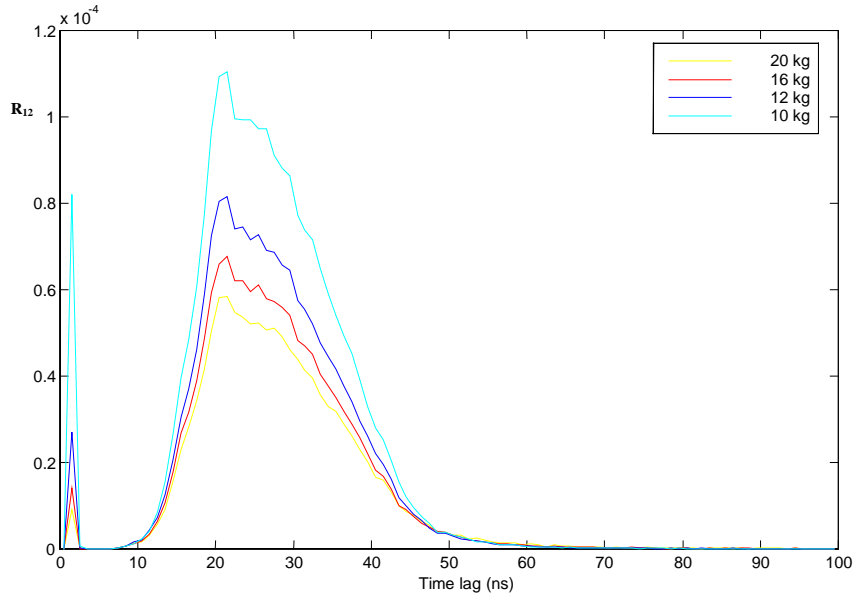


Fig. 2.2. Source-Detectors Cross Correlation Function ( $R_{12}$ ) for Uranium Cylinders of Varying Masses and Fixed Enrichment (36 % wt  $^{235}\text{U}$ ).

### 3. SELECTION OF FEATURES FOR THE SAMPLE IDENTIFICATION ALGORITHM

The selection of features for the sample identification algorithm (SIA) was performed on the basis of their relationship to sample attributes and of their ability to discriminate between close numerical values within each attribute group.

The first feature ( $F_1$ ) chosen is the integral of the cross-correlation function at time lags from 0 to 8 ns, normalized to the same integral of the void calculation. It essentially corresponds to the normalized area of the first peak of the cross-correlation function.  $F_1$  depends only on the sample mass.

The second feature chosen ( $F_2$ ) is the integral of the cross-correlation function at time lags from 0 to 100 ns, normalized to the same integral of the void simulation.  $F_2$  is sensitive to both the sample's total mass and

enrichment. The moments of the cross correlation function were also examined, however, up to  $n=3$ , all the moments examined looked very much alike, with the  $n=1$  moment giving the best resolution. Hence, the average delay time,  $\bar{\tau}$ , was selected as the feature ( $F_3$ ). This feature is essentially constant for the depleted samples, increases with sample enrichment and for high enrichments is very sensitive to sample mass. Because the asymmetry of the second peak is generated by the neutron-induced fission in the sample, the skewness of the cross correlation function was selected as feature ( $F_4$ ).  $F_4$  is especially sensitive to the lower values of enrichment of the samples.

#### 4. APPLICATION OF NEURAL NETWORKS TO NUCLEAR MATERIALS IDENTIFICATION SYSTEMS

Two three-layered artificial neural networks<sup>4, 5, 6</sup> were trained to generate a mapping from input ( $F_1, F_2, F_3$ , and  $F_4$ ) to output (sample's mass and enrichment). The well-known error back-propagation algorithm was used for the network's training. The activation functions were chosen to be sigmoidal from the input to the hidden layer and linear from the hidden layer to the output. The number of hidden nodes was set to two.

For each NN, the values of learning rate and momentum for the training were optimized by a genetic algorithm (GA)<sup>7</sup> (the choice of these parameters is usually made by a trial and error approach). In the GA an initial population of 50 chromosomes each made up of two genes coding the quantities of interest, is allowed to evolve according to the rules of mating, cross-over, and mutation, similarly to what occurs in biological systems. The objective is to maximize the fitness function, defined as the inverse of the NN's training error. After a predetermined number of generations (100 in our case), the fittest chromosome is elected.

The values of learning rate and momentum selected as described above were then used in training the neural networks for the prediction of the total mass and enrichment of the samples on the basis of the four features  $F_1$ - $F_4$ .

Having chosen a linear transfer function in the output nodes of the NN allows us to express the network mapping structure in terms of the simple analytical formula

$$Output = \frac{a_1}{1 + e^{-\left(\sum_{i=1..4} b_i F_i + b_5\right)}} + \frac{a_2}{1 + e^{-\left(\sum_{i=1..4} c_i F_i + c_5\right)}} + a_3$$

where  $a_i$ , ( $i=1,2,3$ ),  $b_j$ ,  $c_j$ , ( $j=1,\dots,5$ ) are coefficients which depend on the network's weights, and the output is the sample mass and enrichment.

19 simulations, about two-thirds of the data available, were selected for the NN training, while the remaining 11 cases were used for testing. Figures 4.1 – 4.2 show the sample mass and enrichment predictions obtained with the NN-GA approach for the test set. Inspection of these figures shows that the present type of neural network can predict enrichment and mass values for uranium metallic cylinders and spheres to a very good approximation.

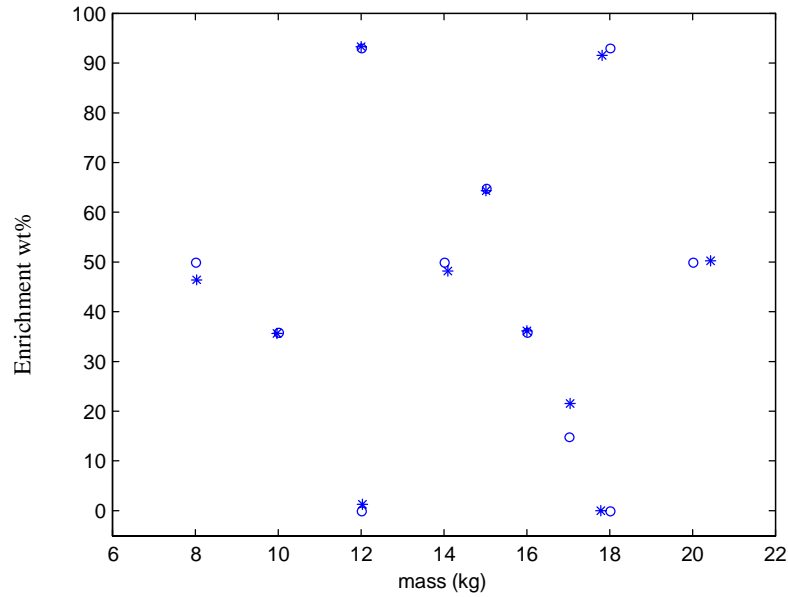


Fig. 4.1. Neural Network Prediction of Mass and Enrichment on the Basis of Features  $F_1$ ,  $F_2$ ,  $F_3$ , and  $F_4$ : Test Set of 11 Cases Relative to Cylinder Simulations. The True Values are Shown with the Circles and the Values Predicted by the Network with Stars.

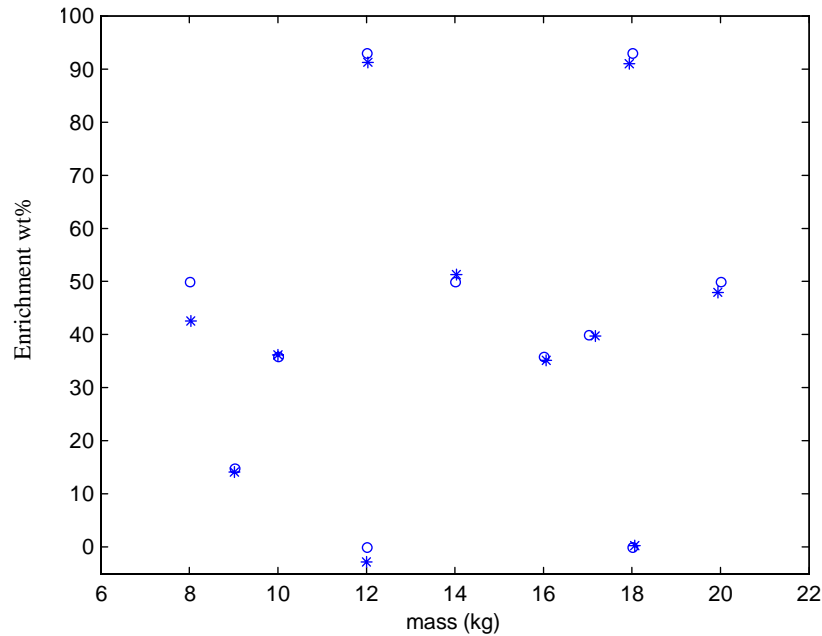


Fig. 4.2. Neural Network Prediction of Mass and Enrichment on the Basis of the Features  $F_1$ ,  $F_2$ ,  $F_3$ , and  $F_4$ : Test Set of 11 Cases Relative to Sphere Simulations. The True Values are Shown with the Circles and the Values Predicted by the Network with Stars.

## 5. APPLICATION OF GENETIC PROGRAMMING TO NUCLEAR MATERIALS IDENTIFICATION SYSTEMS

Genetic Programming (GP) is an evolutionary computation technique that is able to evolve Lisp programs<sup>8,9</sup> to perform various tasks. A mathematical expression (just a Lisp sentence) can be easily expressed in the

form of a parse tree. GP technique practitioners use it to solve regression problems, i.e., problems in which a data set in the form of pairs

$$\{X_i, Y_i\}$$

describe a sampling of the mathematical expression

$$Y = f(X).$$

GP is used to get an explicit mathematical expression for the function  $f$  with the unique information given by the data set. The algorithm performs operations such as reproduction, mutation, and crossover, on the initial population producing a new population. Hopefully this will include new members which, on average, will outperform the previous population when solving the problem. The process is repeated many times, and usually a new member is created that totally solves the problem.

The GP algorithm was applied to generate a function mapping the features,  $F_1$ ,  $F_2$ ,  $F_3$ , and  $F_4$ , to the sample mass and enrichment.

The following equations show one example of results obtained for each sample (note that the features and desired outputs were normalized). Many solutions with an acceptable error were generated, and this selection was not made under any objective criteria.

CYLINDER:

$$\text{Mass} = (((((F1 - -0,514) * ((F1 - (((F1 * F1) - F1) + -0,876) / (-0,502 + -0,584))) * -0,58)) * -0,582) * -0,574) - (((-0,876 - F1) + ((F1 * (((F1 * F1) - F1) + -0,882) / (-0,49 + -0,544))) * (F1 * F1))) / (-0,498 + -0,59)))$$

$$\text{Enrichment} = (((F4 - (-0,014 * (F4 - (-0,014 / F4)))) - (((F2 * 0,748) * ((F3 * 0,366) + (F4 - (-0,014 / ((F1 + ((F4 - (-0,014 / (F2 - (F4 * F3)))) - (-0,014 * F4))) - (F4 * (F3 / 0,748)))))) * F3)) + F2)$$

SPHERE:

$$\text{Mass} = ((-0,204 * ((F2 * (((-0,49 * ((F4 - -0,722) - (F2 * ((-0,49 / -0,88) + F2)))) * (-0,45 / (((F3 * F2) * ((F2 * F2) - F2)) * ((F3 * -0,722) - F2)) - F2)) - F2)) - F3)) - F2)$$

$$\text{Enrichment} = ((((-0,5 + (F4 + (F2 * (F4 - F3)))) * F2) * (F4 * -0,742)) - ((F4 * -0,49) + (((F4 + F2) - (-0,496 + ((F4 - (((F4 - F3) - -0,81) * ((F4 - F3) * (F4 + F2))) * F4)) * -0,49))) + F2) * -0,54)))$$

The constants that are found in each equation were created in the initial population and passed from tree to tree at each iteration of the algorithm through the application of the genetic operators. One of the major achievements of the GP when solving a regression problem is how it manages to combine constants to create new ones.<sup>8</sup>

After inspection of the above equations, it can be found that:

- a). Mass for the cylinder is calculated using just  $F_1$ . This simplification can be found in most of the solutions. The explanation of this result is that the cylinder intercepts most of the source photons, thus, the area under the photo peak, normalized to the same area for the void run, is a measure of the photon attenuation that depends on the sample mass. Because for cylinders, the  $F_1$  feature depends so strongly on the mass of the sample, the GP program selected just  $F_1$  among the four inputted features.

- b). Mass for the sphere is calculated using just  $F_2$  and  $F_3$ . We have found this kind of simple dependence in many other solutions. The spherical sample intercepts less photons than in the case of the cylindrical sample, thus,  $F_1$  does not contain too much sample mass information. The  $F_2$  feature, on the contrary, contains the mass information from the photo peak ( $F_1$ ), plus the sensitivity to sample mass imprinted in the left side of the second peak. The third feature,  $F_3$ , is also selected by the program for its high sensitivity to sample mass at high sample enrichments.

For both spherical and cylindrical samples, the equations constructed by the GP algorithm to determine the sample enrichment depend only on the  $F_2$ ,  $F_3$ , and  $F_4$  features because of the  $F_1$  feature exclusive dependence on sample mass.

For both samples the mass prediction is very accurate in and out of the training set. The sample enrichment prediction is within a 4% band for enrichments above 15%. The error increases as the enrichment decreases towards the depleted case. A significant property of the (GP) algorithm is its capability to select and then combine in an explicit fashion a given set of features for optimal attribute determination.

## 6. COMPARISON OF RESULTS

In order to make a more meaningful comparison of the results we applied a standard regression to predict the mass and enrichment of the cylindrical and spherical samples. Tables I and II summarize the error for the three techniques for both training and test cases. The error measure used is:

$$Error = \frac{\sum_i |real_i - predicted_i|}{\sum_i real_i}$$

Table I: Error Results for the Cylindrical Samples.

Cylinder	PREDICTED BY GP		PREDICTED BY NN		PREDICTED BY Regression	
	MASS	ENRICH	MASS	ENRICH	MASS	ENRICH
Training	0.71%	1.67%	0.22%	2.07%	3.05%	14.81%
Test	1.34%	2.16%	0.81%	2.14%	2.69%	12.68%
Extra	0.45%	8.18%	0.13%	9.05%	1.87%	10.52%

Table II: Error Results for the Spherical Samples.

Sphere	PREDICTED BY GP		PREDICTED BY NN		PREDICTED BY Regression	
	MASS	ENRICH	MASS	ENRICH	MASS	ENRICH
Training	0.17%	2.95%	0.27%	2.20%	1.95%	21.37%
Test	0.15%	2.38%	0.27%	4.59%	2.18%	14.71%
Extra	0.38%	14.00%	0.72%	13.33%	1.08%	43.40%

The tables show that NN and GP are comparable and more effective than a regression in solving the prediction problem. NN and GP are capable of dealing with non-linear problems and this is demonstrated in the case of the enrichment for both configurations, cylinder and sphere, in which the linear solution, the regression, performs very poorly, indicating that the problem is strongly non-linear.

We have found non-remarkable differences in the performance between the artificial intelligence techniques. Two cases (rows labeled as 'Extra' samples in Tables I and II) of the test sets had enrichment and mass values selected outside of the training set range. These can be used to test the overfitting of the models. The error in predicting these enrichment values range from 8% to 14%, indicating that there has been some overfit. This can be explained by considering that there were only four values of enrichment in the training set, covering a wide range of enrichment: from deplete to highly enriched uranium. The error in predicting the mass values is below 1%.

## 7. SUMMARY AND CONCLUSIONS

Monte Carlo simulations of the source-detector cross correlation function for various sample shapes, mass and enrichment values have been performed to serve as a training set for two artificial intelligence algorithms (AI), neural networks (NN), and genetic programming (GP). The input presented to the AI algorithm has been in the form of features extracted from the physical properties of the cross-correlation functions related to mass (beam attenuation) and to enrichment (fission induced pulse broadening). Both the NN and GP algorithms have shown good capabilities and robustness for mass and enrichment predictions of uranium metal samples.

These results serve as a proof of principle for the application of combined stochastic and AI methods to safeguards procedures.

## ACKNOWLEDGMENTS

We would like to thank Prof. R. B. Perez, Prof. J. T. Mihalczo, Dr. T. E. Valentine, and Dr. J. K. Mattingly of the Instrumentation and Controls Division, Oak Ridge National Laboratory and Prof. M. Marseguerra, of the Department of Nuclear Engineering, Polytechnic of Milan, for their valuable intellectual contributions and experienced guidance.

## REFERENCES

1. J. T. Mihalczo, T. E. Valentine, J. A. Mullens, and J. K. Mattingly, Report Number Y/LB-15,946 R3, September 26, 1997.
2. M. S. Krick, D. G. Langner, et. al., *Nuclear Material Management* (Proc. Issue) XXI, 779 (1992).
3. T. E. Valentine, "MCNP-DSP Users Manual", ORNL/TM-13334, Oak Ridge Nat. Lab, January 1997.
4. D. E. Rumelhard and J. L. McClelland, *Parallel Distributed Processing*, Vol. 1, MIT Press, Cambridge, MA (1986).
5. M. Marseguerra, S. Minoggio, A. Rossi, and E. Zio, "Artificial Neural Networks Applied to Multiple Signals in Nuclear Technology," *Progress in Nuclear Energy*, Vol. 27, **4** (1992).
6. R. E. Urig, "Potential Application of Neural Networks to the Operation of Nuclear Power Plants," *Nuclear Safety*, Vol. 32, **1** (1991).
7. L. Chambers, *Practical Handbook of Genetic Algorithms – Applications*, CRC Press (1995).
8. J. R. Koza, *Genetic Programming: On the Programming of Computers by Means of Natural Selection*, MIT Press (1992).
9. J. R. Koza, *Genetic Programming II: Automatic Discovery of Reusable Programs*, MIT Press (1994).
10. P. J. Angeline, *Genetic Programming and Emergent Intelligence*, K. E. Kinnear, Jr., Editor, *Advances in Genetic Programming*, MIT Press (1994).
11. W. Banzhaf, P. Nordin, R. E. Keller, and F. D. Francone, *Genetic Programming: An Introduction* (1998).